



# Nuclear performance assessment of ARIES-AT

L.A. El-Guebaly\*, The ARIES Team

*Fusion Technology Institute, University of Wisconsin-Madison, 1500 Engineering Drive, Madison, WI 53706, USA*

Accepted 1 June 2005

Available online 10 October 2005

## Abstract

The transition to a new ARIES design always involves a significant change in the engineering system with emphasis on high performance. Compared to ARIES-RS, numerous improvements were noted in ARIES-AT, ranging from physics improvements to a focus on advanced engineering for an economically and environmentally attractive source of energy. During the course of the ARIES-AT study, we closely monitored the key nuclear parameters and called for measures to enhance the engineering and physics aspects of the design. Optimization of components' constituents, characterization of the radiation environment, and meeting the ARIES-AT specific design needs were also given considerable attention. A key engineering aspect of ARIES-AT is its compactness and the high-conversion efficiency (~60%) of the LiPb/SiC blanket that is capable of performing at high temperature (~1000 °C). Certain features of the nuclear activity were focused on areas unique to ARIES-AT, including breeding potential of the LiPb/SiC blanket containing tungsten stabilizing shells, high-performance shielding components to protect the high-temperature superconducting magnet, and compact radial builds to minimize the volume of solid waste requiring near-surface geological burial. The final design satisfies the top-level requirements and no serious nuclear issues have been identified for ARIES-AT. A salient design feature is the significant reduction in the ARIES-AT radwaste volume relative to precedent designs developed since the inception of the ARIES project in the late 1980s. Design measures such as the high-power density, well optimized shield, and blanket segmentation with extended service lifetime have all contributed to the waste minimization.

© 2005 Elsevier B.V. All rights reserved.

## 1. Introduction

Promising advances in tokamak physics and fusion technology (derived from national and worldwide developmental and experimental programs) enhanced the performance of the most recent ARIES design

and ensured its competitiveness with other power generation systems. The 1000 MW<sub>e</sub> ARIES advanced tokamak (AT) design [1] is safer, economical, more compact, and therefore generates less radioactive waste compared to predecessor designs. As Fig. 1 indicates, the internals of ARIES-AT are the standard tokamak components, namely the blanket, shield, vacuum vessel, and magnets. The design is built on the ARIES-RS study that relies on reversed-shear

\* Tel.: +1 608 263 1623; fax: +1 608 263 4499.

E-mail address: [elguebaly@engr.wisc.edu](mailto:elguebaly@engr.wisc.edu).

## Cross Section of ARIES-AT Power Core Configuration

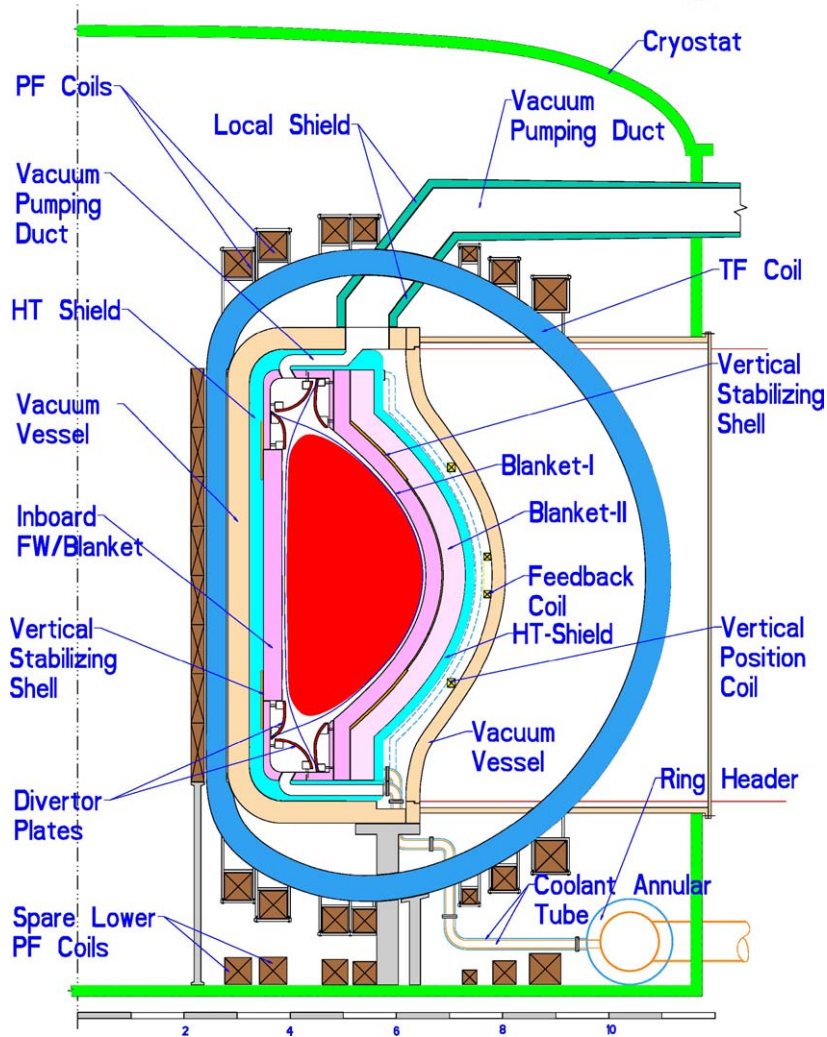


Fig. 1. ARIES-AT vertical cross section.

(RS) physics, focusing on more advanced physics and technology. Several important features have been incorporated to improve the performance of ARIES-AT. For instance, the high-temperature SiC/SiC structure operates at 1000 °C, the high-performance blanket achieves ~60% efficiency, the near plasma stabilizing shells allow high plasma- $\beta$  exceeding 10%, the radiation-resistant high-temperature superconducting magnets offer less stringent radiation limits, and the high-performance shield results in more compact radial builds that help minimize the radwaste.

Table 1 summarizes the key design parameters and radiation limits that are essential for the nuclear assessment. The neutron wall loading profile resembles that of ARIES-RS [2] with slightly lower values mainly due to the increased thermal conversion efficiency. The distribution peaks at the outboard (OB) midplane at ~4.8 MW/m<sup>2</sup> and drops to ~1 MW/m<sup>2</sup> at the divertor plates. In absence of firm experimental data for advanced structural materials and high-temperature magnets, optimistic criteria determined the limits and accounted for future improvements to existing materi-

als. This certainly represents an important issue open to debate between materials experts and designers.

During the 2-year term of the study, the nuclear analysis has been a fundamental element of the design process. In addition to the continuous updates of the neutronics and shielding performance, we were actively involved in the design development and provided attractive options for self-sufficient tritium breeding blanket, well-optimized shield, compact radial build, acceptable radiation damage to structural components, and reasonable service lifetime for in-vessel components.

## 2. Key nuclear objectives and requirements

We began the nuclear assessment by identifying a set of nuclear objectives in support of the top-level requirements developed in the mid-1990s for the ARIES power plants [3]. These are summarized below:

Top-level requirements	Nuclear-related impact <sup>a</sup>
Closed tritium fuel cycle	Calculated TBR $\geq 1.1 \Rightarrow$ net TBR $\geq 1.01$
Low-level waste	Careful choice of low activation materials
Structural integrity	W-based materials in outer components only No hydrides in shield
Minimum waste	Well-optimized components Compact radial build Segmented blanket
Competitive COE	Efficient WC filler for IB side to reduce machine size SiC structure for inner HT components only Less expensive FS structure for outer LT components

<sup>a</sup>Acronyms: TBR, tritium breeding ratio; COE, cost of electricity; IB, inboard; HT, high-temperature; LT, low-temperature; FS, ferritic steel.

A tritium-breeding ratio (TBR) of 1.1 assures tritium self-sufficiency for ARIES-AT. The 10% breeding margin accounts for the uncertainties in the cross section data ( $\sim 7\%$ ), approximations in geometric model ( $\sim 2\%$ ), losses during T reprocessing ( $\sim 1\%$ ), and T supply for future power plants ( $\sim 1\%$ ). Ref. [4] provides a more detailed breakdown of the breeding margin. The net TBR at the beginning of plant operation may range between 1.01 and 1.2 and a flexible blanket design could adjust the net TBR to 1.01 after

Table 1  
Key design parameters and radiation limits for ARIES-AT

Fusion power	1755 MW
FW location	
Midplane—IB, OB	3.85, 6.55 m
Top/bottom—IB, OB	3.85, 4.7 m
Neutron wall loading	
Peak at IB, div., OB	3.1, 2, 4.8 MW/m <sup>2</sup>
Average at IB, div., OB	2.2, 1, 4 MW/m <sup>2</sup>
Machine lifetime	40 FPY
Availability	80%
SiC burnup limit	3%
FS dpa limit	200 dpa
FS reweldability limit	1 He appm
HT magnet fluence limit	$10^{19}$ n/cm <sup>2</sup> ( $E_n > 0.1$ MeV)
GFF polyimide insulator limit	$10^{11}$ rad

the first blanket changeout. In case of over-breeding (net TBR  $> 1.01$ ), the TBR can be reduced by lowering the enrichment or replacing breeding modules by shielding components. In case of under-breeding (net TBR  $< 1.01$ ), major changes are needed to adjust the breeding. These include replacing the W stabilizing shells by Al or Cu shells, lowering the SiC structure in the blanket, or adding beryllium to the blanket.

Addressing the nuclear issues, it was prudent to routinely check if the requirements are met when the design choices are made and whether there is still further improvement potential. We started the analysis by examining the breeding capacity of the candidate breeders, and then defined the blanket parameters (thickness, composition, and Li enrichment). Next, the shield and vacuum vessel were simultaneously designed to essentially protect the magnets. Finally, we specified the radial build and identified the key nuclear parameters: TBR, neutron energy multiplication ( $M_n$ ), nuclear heat load to all components, radiation damage to structural components and their service lifetimes. The nuclear assessment proceeded inter-actively with guidance from the thermo-mechanical analysis.

## 3. Blanket system modeling and breeder selection

From its very inception, ARIES-AT selected the SiC/SiC composites [5] as the main structure for the

high-temperature components as they can withstand very high temperature ( $\sim 1000^\circ\text{C}$ ), a property of high payoff. Moreover, it is an inherently low activation material with very low decay heat and can easily satisfy the low-level waste requirement [6]. The selection criteria for the breeder include several design parameters that play an essential role in the acceptability of the breeder. These are the compatibility with the SiC structure, tritium-breeding capacity, radiation stability, safety characteristics, operating temperature window, and projected thermal efficiency for the overall system. Two liquid metal (LM) breeders and a molten salt seem to be compatible with the SiC/SiC composites. Those are  $\text{Li}_{17}\text{Pb}_{83}$ ,  $\text{Li}_{25}\text{Sn}_{75}$ , and  $\text{F}_4\text{Li}_2\text{Be}$ . Each breeder has its own design issues that are addressed in detail elsewhere [7–9]. This nuclear assessment examines the breeding potential of the three breeders. Two blanket designs were originally proposed for ARIES-AT: a self-cooled LM concept and a dual-coolant (He and LM) concept. Further development and investigation were carried out to underpin the design choices and led to the selection of the self-cooled concept as the reference design as it outperformed the dual-cooled concept. In the reference design, the LM flows poloidally upward through the FW, returns downward in the blanket cells, and exits the blanket at  $\sim 1100^\circ\text{C}$ , allowing a high thermal conversion efficiency of  $\sim 60\%$  with the Brayton cycle [7].

Three-dimensional Monte Carlo analysis was performed using the MCNP code [10] to confirm the key nuclear parameters. Preceding the 3D analysis, a series of parametric 1D analysis using the DANTSYS code [11] was established to guide the design process. The 1D estimate is based on coupling the 1D results with the neutron coverage fraction of the blanket segments. Use is made of the 3D results to re-normalize the neutron source for the 1D analysis. The FENDL-2 data library [12] was employed for both analyses, point-wise data for the 3D analysis and 175 neutron and 42- $\gamma$  group structure for the 1D analysis with  $P_3$ – $S_8$  approximation. The 3D model included the essential components comprising the power core: the first wall (FW), blanket, shield, stabilizing shells, divertor, and magnets (see Fig. 1). The innermost cell of the blanket was modeled separately as it controls the breeding level. The 10,000 source particles resulted in acceptable statistical errors of  $<5\%$  for FW local damage and heating and  $<1\%$  for overall TBR and  $M_n$  parameters. Excellent agree-

ment was obtained between the 1D and 3D estimates for TBR and  $M_n$  [13].

The breeding potential of all breeders (90% enriched  $\text{Li}_{17}\text{Pb}_{83}$ , 90% enriched  $\text{Li}_{25}\text{Sn}_{75}$ , and natural  $\text{F}_4\text{Li}_2\text{Be}$ ) was examined using the LiPb/SiC FW and blanket configuration [7]. Even though the  $^6\text{Li}$  enrichment enhanced the TBR of LiPb and LiSn breeders, it degraded the breeding of the FLiBe system. The results showed that the TBR of the LiSn/SiC and FLiBe/SiC blankets remained below 0.9 and the breeding requirement (1.1) could not be met even with a fairly thick blanket. The lack of breeding has ruled out the LiSn and FLiBe breeders from further consideration. Both breeders will certainly need a beryllium multiplier to provide a TBR of 1.1. Beryllium may raise safety, economic, and resource concerns that need further investigation.

There is only one blanket segment on the inboard (IB) side, whereas on the outboard side there are two segments, the outer segment being designed as a lifetime component. The segmentation helps reduce the cumulative blanket waste and replacement cost by a factor of 2. Originally, the thickness of the IB segment was set at 30 cm and those of the two OB segments at 30 and 35 cm, which for the following material selection (20% SiC structure in blanket, 90% enriched LiPb, 4 cm thick W vertical stabilizing shells, necessary assembly gaps between 16 modules, and 2.5 m<sup>2</sup> penetrations) resulted in an overall TBR of 1.1. The IB blanket, OB blanket, and both shield and divertor system supply about 25%, 70%, and 5% of the breeding, respectively. However, incorporation of the latest stabilizing shell design was found to reduce the overall TBR below the 1.1 requirement. This can mainly be compensated by increasing the thickness of the blanket, as discussed in the next section. Enriching the LiPb above 90% would increase the TBR by about 1% but would not be cost effective.

#### 4. Impact of stabilizing shells on breeding

A specific topic that has been investigated jointly by the engineers and physicists is the location of the stabilizing shells and their impact on the physics parameters ( $\beta$ , elongation, plasma current, and triangularity) and nuclear parameters (TBR, nuclear heating, activation, and decay heat). We suggested moving the OB shells closer to the plasma and placing them between the

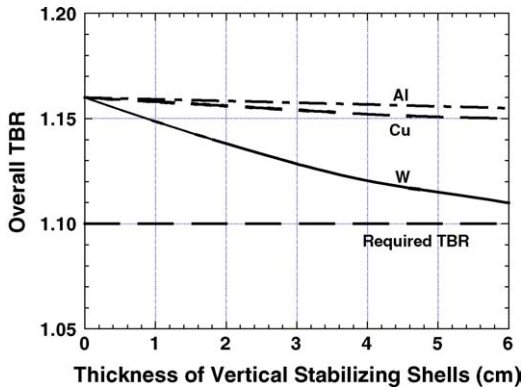


Fig. 2. Degradation of TBR with thickness of vertical stabilizing shell for 35 cm thick IB blanket and 75 cm thick OB blanket.

two OB blanket segments instead of behind the blanket, as defined in the previous ARIES-RS design [14]. This suggestion had a favorable impact on the plasma physics resulting in a triangularity of 2.2 and a high- $\beta$  of 10% or more [15]. However, the nuclear analysis indicated that the OB shells would deteriorate the breeding to a TBR < 1.1, depending on the exact shell configuration (dimension, material, and location). A design solution would be to increase the OB blanket thickness to compensate for the losses in breeding if the TBR is unacceptably low. For example increasing the IB blanket region thickness to 35 cm and the second OB blanket region to 45 cm would restore an overall TBR of 1.1. For consistency, this was used as the basis for all neutronics, safety, and economics analyses.

Three candidate vertical shell materials (W, Cu, and Al) have been investigated. As illustrated in Fig. 2, an Al conductor has the least impact on breeding followed by Cu, then W. The thickness of the shell depends on the type of conductor, operating temperature, and time constant. Further optimization analysis indicated that W is the preferred material for the shells that operate hot and are passively cooled. The toroidally continuous OB vertical stabilizing shells are placed at the upper/lower extremity of the OB blanket ( $z = 1.8\text{--}2.8$  m). The local breeding in the OB blanket behind the 4 cm thick W shells dropped by up to  $\sim 40\%$ , which is a 4% reduction in the overall TBR. The 1 cm thick resistive wall mode (RWM) shell located at the OB midplane between the vertical shells dropped the breeding further by  $\sim 2\%$ . No outstanding safety issues were identified for the W shells [6]. The decay heat is minimal due to the small

volume of the shells and the outer blanket segment containing the shells still qualifies as Class C waste at the end of plant operation.

## 5. Radial build definition

Discussed in the following sections is the in-vessel component optimization process that helped define the operational space of the machine, therefore minimizing the burden of unnecessary waste generated by non-optimized radial builds. During this process, we focused our shielding effort on the inboard area where a better shielding performance makes a notable difference to the overall machine size. We placed less emphasis on the outboard and divertor areas where the shielding space is not constrained and no economic and design enhancements are gained with high-performance, compact shields.

The inboard, divertor, and outboard radial builds used for the neutronics and safety calculations are shown in Figs. 3–5, respectively, highlighting the main features of the blanket, shield, vacuum vessel, and TF magnet. The water-cooled vacuum vessel (VV) is a low-temperature (LT) component and the LiPb-cooled shield is a high-temperature (HT) component. The gap between the VV and magnet contains 15% thermal superinsulation. An interim design had a thin LT shielding component located between the HT shield and a thin VV, analogous to ARIES-RS [4]. With close collaboration with the VV designers, we suggested combining the LT shield and VV in a single unit due to common materials, similar lifetimes, and structural connections. This would also simplify the plumbing connections and

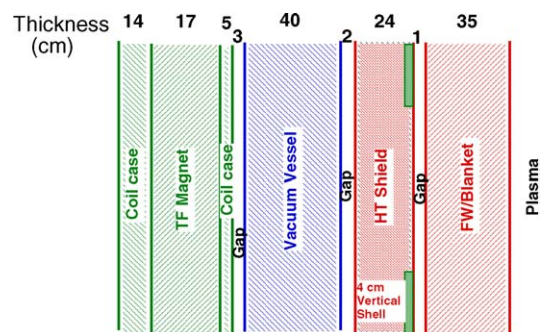


Fig. 3. Inboard radial build of ARIES-AT.



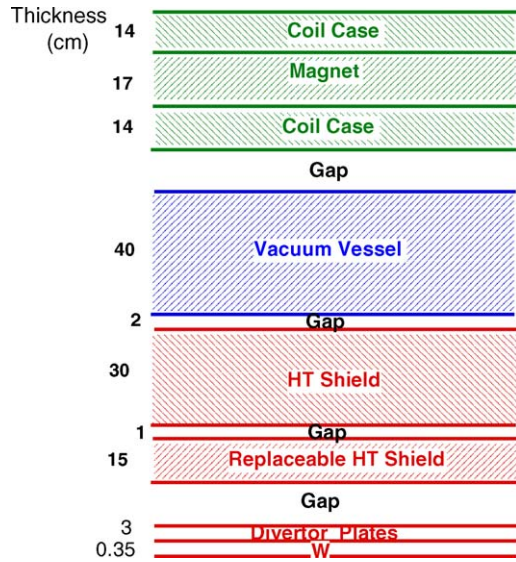


Fig. 4. Vertical build of ARIES-AT.

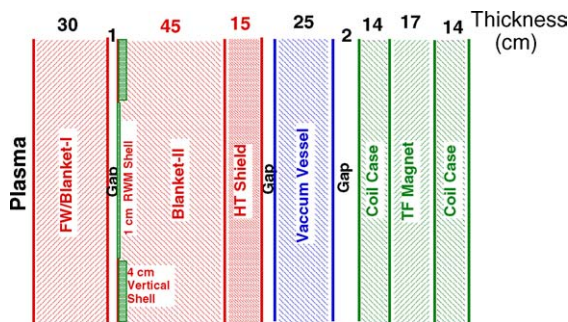


Fig. 5. Outboard radial build of ARIES-AT.

increase the structural integrity of the VV. The only problem is that if there is a need to cut and weld the VV during the plant life, the welds must be protected from radiation.

## 6. Magnet protection requirements

We revisited the magnet radiation limits as they strongly influence the compositions and size of the shielding components. All in-vessel components (blanket, shield, and VV) provide a shielding function for the magnets. As discussed later, the composition of the outermost component (VV) is driven partly by magnet shielding considerations. The selected conductor

material for both the TF and PF coil sets [16] is the  $\text{YBa}_2\text{Cu}_3\text{O}_5$  (referred to as YBCO) because of the low material unit cost and inexpensive construction technique (\$50/kg). The liquid nitrogen-cooled coils are dominated by the Inconel structure (72%) and can operate at high fields ( $>16\text{T}$ ) without a quench requirement [17]. The cooling requirement for the YBCO HT magnet is greatly relaxed compared to the liquid helium-cooled magnets of ARIES-RS because of the higher operating temperature (70–80 K). This means the nuclear heat limit to the HT magnets could be quite high and the cryogenic heat load is not a concern [17]. The limit for the glass-fiber-filled (GFF) polyimide insulator is  $10^{11}$  rads, same as for ARIES-RS [2]. Therefore, the predominant radiation limit is the fast neutron fluence to the YBCO conductor. With the limited irradiation data presently available, the magnet designers predict the radiation limit for the YBCO conductor to be comparable to the limit for the  $\text{Nb}_3\text{Sn}$  conductor, that is,  $10^{19}$   $\text{n}/\text{cm}^2$  for  $E_n > 0.1$  MeV [17].

## 7. Vacuum vessel design and trade study

Being the closest component to the magnet, the VV composition greatly influences the magnet radiation effect. The skeleton of the double-walled VV with internal ribs provided by the VV designers [18] was filled with shielding materials and optimized to achieve the necessary requirements for magnet shielding. Tradeoff analyses of the water and filler materials were conducted for the VV. We had two candidates for consideration: a high-performance design using tungsten carbide (WC) filler and a more typical borated ferritic steel (B-FS; FS with 3 wt.% B) design. The WC-based inboard shield and VV is 15 cm thinner than a B-FS-based design. An optimal combination for the VV would be to use WC for the inboard to reduce the size of the overall machine, B-FS for the divertor, and only water for the outboard to simplify the VV design. The IB/divertor and OB sections of the VV call for 13% and 30% FS structure, respectively, dictated by the structural requirements of the VV [18]. Figs. 6 and 7 demonstrate the VV optimization curves, showing the tradeoff between water and filler. About 22% water is optimal for the IB VV section, driven by shielding considerations. For simplicity, the same water content is used in the divertor section. Even though the OB VV

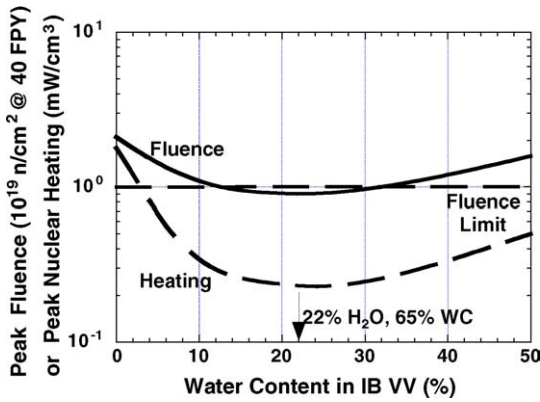


Fig. 6. Variation of radiation effects at TF coil with compositions of IB section of W, substituting WC for water.

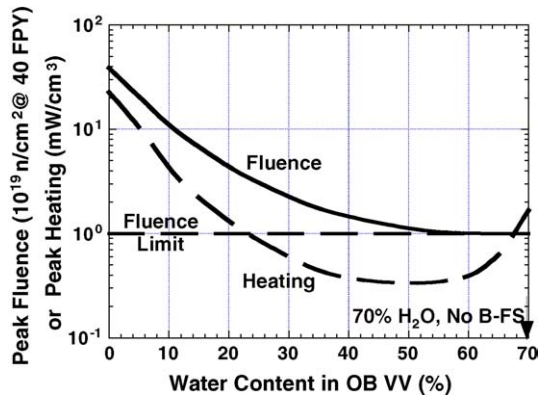


Fig. 7. Impact of VV composition on radiation effects of outer legs of TF coils, substituting B-FS for water.

section optimizes at 50–70% water (see Fig. 7), a decision was made to eliminate the filler to simplify the OB VV design. The 70% water content results in notably higher magnet heating and VV activation [6]. It is noted that the elimination of the B-FS filler has increased the VV neutron flux with  $E < 1$  keV by several orders of magnitude.

Table 2  
Peak radiation effects at TF magnet

	IB	OB	Divertor	Limit
Fast neutron fluence ( $E_n > 0.1$ MeV) ( $n/cm^2$ @ 40 FPY)	$9 \times 10^{18}$	$1 \times 10^{19}$	$9 \times 10^{18}$	$10^{19}$
Nuclear heating ( $mW/cm^3$ )	0.2	1.7	0.2	–
Dose to GFF polyimide (rad @ 40 FPY)	$7 \times 10^9$	$3 \times 10^{10}$	$6 \times 10^9$	$10^{11}$

## 8. Rationale for shield design selection

As an essential element of the power core, the shield provides radiation protection for the externals and meets the power production requirements. The 12% nuclear heating carried out by the shield is recovered to enhance the power balance and economics. Therefore, the shield operates hot and employs 15% LiPb for cooling and B-FS as filler. Substitution of the B-FS with WC would have decreased the IB radial build by  $\sim 5$  cm but generates higher decay heat by an order of magnitude. Correspondingly, the temperature rise during an accident is also higher by one or two orders of magnitude, depending on the time period after the onset of the accident. Therefore, we avoided the use of WC filler in the shield for safety reasons and recommended the use of B-FS filler instead. Note that the innermost component of the divertor shield employs FS filler to control the tritium inventory. Overall, the shield and VV design choices help improve the economics and reduce the radiation damage at the magnets below the allowable radiation limits. Table 2 provides the radiation level at the TF magnet for the base case design. In all 1D shielding calculations, we have considered a safety factor of three to account for uncertainties in the computing tools and design elements. The main features of the shielding system could be summarized as follows:

- HT and LT components to reduce cost [2].
- Nuclear heating recovered ( $\sim 12\%$ ) to improve power balance.
- SiC structure and LiPb coolant for HT shield.
- Less expensive FS structure with water coolant for LT VV.
- Fillers with SiC and FS structures to improve shielding and reduce cost.
- Highly efficient WC fillers for IB section of VV to reduce machine size.
- Water coolant for VV for better shielding performance.

Table 3  
Composition<sup>a</sup> of ARIES-AT components (in vol%)

	Inboard	Divertor	Outboard
Divertor plates		40% SiC, 50% LiPb, 10% W	
FW/Blanket-I	19% SiC, 81% LiPb		20% SiC, 80% LiPb
Blanket-II			19% SiC, 77% LiPb, 3% W
Replaceable HT shield		15% SiC, 10% LiPb, 75% FS	
HT shield	15% SiC, 10% LiPb, 70% B-FS, 5% W	15% SiC, 10% LiPb, 75% B-FS	15% SiC, 10% LiPb, 75% B-FS
Vacuum vessel	13% FS, 22% H <sub>2</sub> O, 65% WC	13% FS, 22% H <sub>2</sub> O, 65% B-FS	30% FS, 70% H <sub>2</sub> O
Coil case	95% 304-SS, 5% LN		
TF coil	72% Inconel-625, 0.5% Ag, 7% YBa <sub>2</sub> Cu <sub>3</sub> O <sub>5</sub> , 7% CeO <sub>2</sub> insulator, 13.5% GFF polyimide insulator		

<sup>a</sup> SiC, W, and WC are 95% dense. A 1.4 cm thick FW contains 73% SiC and 27% LiPb. GFF polyimide consists of 30 wt.% polyimide and 70 wt.% S-glass.

The optimum compositions for all components are listed in Table 3. The SiC-based wedges underneath the outer legs of the TF magnets should match the optimized composition of the blanket and shield to provide the necessary protection for the coils. Along with the blanket/shield/VV, the 5 cm thick port enclosures and the 5 cm thick side coil cases adequately protect the sides of the outer legs of the TF coils.

With the higher triangularity, the IB divertor slot is virtually eliminated, impacting the design of the IB divertor region and the shield behind. More accurate definition of the headers and plumbing in the divertor region helped estimate the damage to the magnet where the IB shield recesses to accommodate the inner divertor plate (see Fig. 1). Our analysis showed no excessive damage or shielding problems behind the inner divertor plates.

A comparison between ARIES-AT and ARIES-RS [2,14] showed an appreciable reduction of 18–43 cm in the dimension of the in-vessel components and an even higher reduction of 42–56 cm when the magnet is included. The superior shielding performance of the LiPb breeder compared to Li, the ability to use water in the VV, and the thinner HT magnet contributed to the compactness of ARIES-AT. Table 4 tabulates the radial dimensions of the components for both designs. The alloying and impurity elements of the ARIES-AT materials are documented in Reference [19].

Table 4  
Radial dimensions (in cm) of ARIES-AT components compared to ARIES-RS

	ARIES-AT			ARIES-RS		
	IB	Div.	OB	IB	Div.	OB
Divertor plates		3.35			5	
FW/Blanket-I	35		30	20.3		20.3
Gap	1	>5	1		1	1
Blanket-II			45			30
Replaceable HT shield		15		20	20	7
Gap		1		1	1	1
HT shield	24	30	15	26	35	28
Gap	2	2	2	2	2	2
LT shield				28	45	40
Gap				2	>2	>2
Vacuum vessel	40	40	25	20	20	30
Subtotal <sup>a</sup>	102	96	118	120	131	161
Gap	3	>5	>5	5	>5	>5
Inner coil case	5	14	14	3	3	3
Coil	17	17	17	50	50	50
Outer coil case	14	14	14	5	5	5
Total <sup>a</sup>	141	146	168	183	194	224

<sup>a</sup> Minimum gap width considered.

## 9. Nuclear heat load to in-vessel components

The power production components include the FW, blanket, shield, and divertor. Table 5 details the breakdown of the nuclear heating deposited in the in-vessel components. As the table indicates, most of the power



Table 5  
Nuclear heat load (in MW) to ARIES-AT components

	Inboard	Divertor	Outboard	Total
FW and divertor	39	43	96	178
Blanket				1207
Blanket-I	302	–	727	
Blanket-II	–	–	178	
HT shield	40	112	9	161
Total	381	155	1010	1546

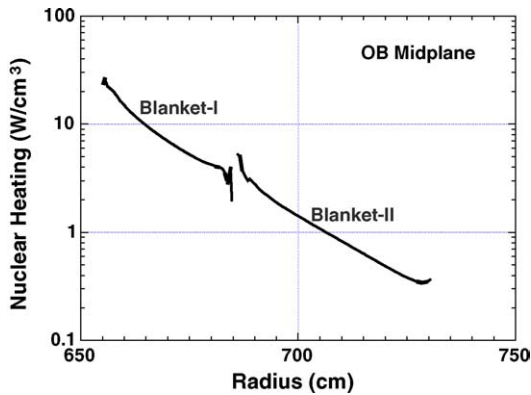


Fig. 8. Radial distribution of nuclear power density in OB blanket.

(88%) goes to the FW, divertor, and blanket. The small heat leakage to the VV (<1%) is dumped as a low-grade heat. The heat load to the TF magnets is  $\sim 50$  kW, corresponding to a LN cryogenic load of  $\sim 0.5$  MW. The IB, divertor, and OB regions generate 25%, 10%, and 65% of the total heating, respectively. For a neutron power of 1404 MW (80% of the fusion power), the neutron energy multiplication amounts to 1.1. The total heat deposition along with the power density distribution shown in Fig. 8 served as a source term for the detailed thermal analysis carried out for the ARIES-AT design [7].

## 10. Lifetime assessment

The ability to identify the life-limiting criteria for the structural materials is a key factor to determine accurately the service lifetime of the in-vessel components. Historically, the thermal and mechanical stresses, thermal creep, burnup of atoms, atomic displacement, and activation products have led to either a failure mech-

anism or a violation of the waste requirement, therefore prematurely ending the service lifetime of structural components. There are no firm guidelines for the SiC/SiC composites [5] while for the FS components, the life-limiting criterion has traditionally been the displacement of atoms, ranging between 100 and 200 dpa. In the ARIES study, we have adopted the limits of 3% burnup for the SiC structure and 200 dpa for the FS structure [2].

Unlike metals, the helium production in SiC is excessive. Another unique feature for SiC is the high He to H ratio of 2–3. Helium could have an adverse effect on the thermal conductivity and mechanical and dimensional stability of the SiC structure. Under ARIES-AT operating conditions, the peak damage to SiC reaches 4200 He appm/FPY, 1700 H appm/FPY and 56 dpa/FPY at the midplane of the OB first wall. Energetic neutrons having  $E > 3$  MeV transmute the Si and C via  $(n, \text{He})$  and  $(n, \text{H})$  reactions into Al, Mg, Li and Be. Each  $(n, \text{He})$  or  $(n, \text{H})$  reaction with either a Si or C atom could potentially burn a SiC molecule. Our results show that Si atoms burn faster than C atoms at a 2:1 ratio. For a 3% burnup limit, the FW/blanket lifetime is  $\sim 4$  FPY, implying an end-of-life fluence of  $18.5 \text{ MWy/m}^2$  for the SiC structure. As Fig. 9 indicates, the burnup rate drops rapidly within the LiPb blanket due to the slowdown and interaction of neutrons with Pb generating lower energy neutrons with energy below the 3 MeV threshold for He and H production. Therefore, we segmented the OB blanket into two parts: a 30 cm thick replaceable FW/Blanket-I with a limited

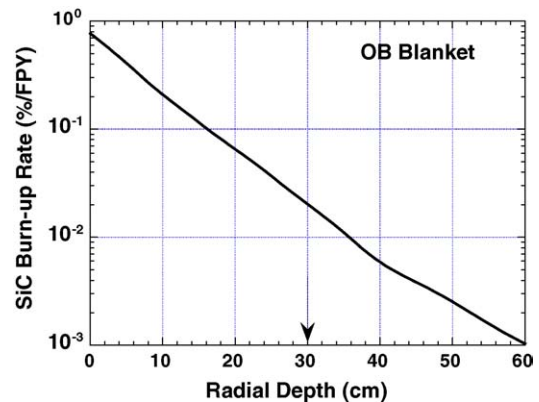


Fig. 9. Radial variation of SiC burnup within the OB blanket reaching the 3% limit at the end of plant life (40 FPY) at a depth of 30 cm.

lifetime of 4 FPY and a permanent 45 cm thick Blanket-II that could last for the entire 40 FPY plant life. This segmentation has lowered the cumulative blanket waste by a factor of 2 and helped reduce the annual replacement cost.

There is a class of low activation, radiation-resistant FS alloys that offer low neutron-induced swelling, low thermal expansion coefficient, high resistance to irradiation creep, and high range of operating temperatures. An example of advanced FS suitable for fusion applications includes MHT-9, F82H, MANET, ORNL-9Cr-2WVTa, and nanocomposited FS. The reference FS for this study is the ORNL-9Cr-2WVTa [20]. The more advanced nanocomposited FS [21] will be considered in future studies. The only FS-based component in ARIES-AT is the vacuum vessel, operating at a nominal temperature of 100 °C. Design measures have been incorporated in ARIES-AT to assure that the maximum temperature during the worst-case accident does not exceed the 700 °C limit, permitting the reusability of the VV following an accident [22]. Regarding the radiation damage, the 200 dpa limit is met at the innermost surface of the VV at the 40 FPY end-of-plant life. However, the FS structure will not survive the high radiation environment if there is a need to cut and reweld the VV during plant operation. For instance, the helium production level at the inner surfaces of the IB and divertor sections of the VV is excessive ( $\sim 15$  He appm @ 40 FPY) and exceeds the project-assumed reweldability limit of 1 He appm for FS. Recently, experimental data for thin 316-SS samples suggested higher limits, ranging from 5 to 30 He appm [23]. Considering today's knowledge of the FS irradiated material properties, the VV welds should be hidden and located away from the high-radiation zones. We proposed a recessed weld joint design that offers sufficient protection if the VV joints need to be rewelded within the nominal service life. Alternatively, we recommend developing a more forgiving FS with higher reweldability limit than 15 He appm to assure rewelding and repairing the VV in-place. The option of replacing the VV with a new component in case of a failure must be carefully examined despite the projected low cost of the VV [18]. The difficult VV replacement could be a prohibitive expense and may require extended shutdown of the machine. The cost of remotely disassemble, relocate, and reassemble the vacuum vessel along with the highly radioactive interior components might

not be cheap and must be weighed against the cost of not operating the plant for failing to repair or reweld the VV.

## 11. Waste minimization

Designing compact radial builds has been recognized as a means to reduce the volume of radioactive waste. Other options for waste reduction include recycling and clearing of materials and components. In advanced designs, only the confinement concrete building would be cleared from regulatory control, not the in-vessel and magnet components [24]. With proper optimization, ARIES-AT has achieved a substantial reduction in the size of the components that contribute to the total volume of radioactive waste. Shown in Fig. 10 is the evolution of the waste volume since the inception of the ARIES project in the late 1980s. The waste volume belongs to the fusion power core components (blanket, shield, divertor, VV, and magnets) documented in the ARIES systems code outputs [25]. Design measures such as high-power density machines, well-optimized radial builds, extended service lifetimes, and segmented blankets have all contributed to the persistent trend in waste minimization. During the 15-year period of the ARIES studies, a fac-

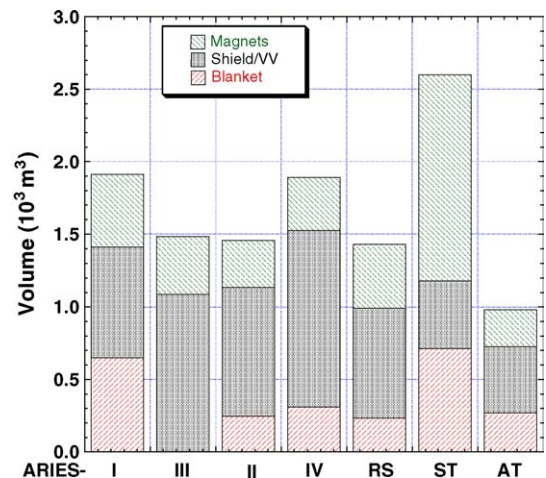


Fig. 10. Evolution of ARIES waste showing a persistent trend in volume reduction for tokamaks (actual volumes excluding replaceable components).

tor of two reduction in waste has been achieved, which is impressive.

## 12. Conclusions

The integrated nuclear activity guided the ARIES-AT design during the design process and interactions with subsystem designers improved the nuclear integration. Most of the nuclear activity was aimed at achieving the desired requirements by focusing effort on the blanket and shielding systems while carefully monitoring the economic and safety impacts of the material choices. A number of breeders were initially considered for ARIES-AT: LiPb, LiSn, and FLiBe. As the design began to develop, it was soon realized that LiSn and FLiBe provide insufficient tritium breeding for the SiC-based system. The reference LiPb/SiC configuration satisfies the minimum breeding requirements ( $TBR = 1.1$ ). As the stabilizing shells were added to the blanket, the excess breeding margin diminished considerably.

All three major components (blanket, shield, and vacuum vessel) provide a shielding function and protect the magnets against radiation. Because of the growing interest in minimizing the volume of waste generated by fusion machines, enhanced shielding features are invoked in this design to avoid a large radial standoff between the plasma and magnet. As a result, ARIES-AT generates the least amount of waste among all ARIES-like tokamaks.

Regarding the radiation damage and service lifetimes, all components except the innermost FW/blanket, divertor system, and front divertor shield are permanent life-of-plant components. The life-limited components need replacement every 4 FPY. The radiation level at the magnet is below the limit. Overall, the material choices for the internals of ARIES-AT satisfy the desired performance requirements and all components are well optimized to achieve the design constraints.

## Acknowledgement

The work was performed under the auspices of the U.S. Department of Energy under contract #DE-FG02-98ER 54462.

## References

- [1] F. Najmabadi and The ARIES Team, The ARIES-AT advanced tokamak, advanced technology fusion power plant, *Fus. Eng. Des.* 80 (2006) 3–23.
- [2] L.A. El-Guebaly, Overview of ARIES-RS neutronics and radiation shielding: key issues and main conclusions, *Fus. Eng. Des.* 38 (1997) 139–158.
- [3] F. Najmabadi, M.S. Tillack, R.L. Miller, T.K. Mau, B.J. Lee, X. Wang, et al., The starlite study: assessment of options for tokamak power plants, University of California-San Diego, UCSD-ENG-005, 1997.
- [4] L. El-Guebaly, Tritium breeding issues for MFE and IFE, Presentation given at Tritium Workshop, Livermore, California, March 6–7, 2001. Available at <http://fti.neep.wisc.edu/FTI/ARIES/MAR2001/tritium.lae.pdf>.
- [5] A.R. Raffray, R. Jones, G. Aiello, M. Billone, L. Giancarli, H. Golfier, et al., Design and material issues for high performance SiC/SiC-based fusion power cores, *Fus. Eng. Des.* 55 (2001) 55–95.
- [6] D. Henderson, L. El-Guebaly, P. Wilson, A. Abdou, Activation, decay heat, and waste disposal analysis for ARIES-AT power plant, *Fus. Technol.* 39 (2, Part 2) (2001) 444–448.
- [7] A.R. Raffray, L. El-Guebaly, S. Malang, I. Sviatoslavsky, M.S. Tillack, X. Wang, Advanced power core system for ARIES-AT, *Fus. Eng. Des.* 80 (2006) 79–98.
- [8] D.K. Sze, R.F. Mattas, Z. Wang, E.T. Cheng, M. Sawan, S.J. Zinkle, K.A. McCarthy, Sn-Li, A new coolant/breeding material for fusion applications, Argonne National Laboratory, ANL/TD/CP-98464, 1999.
- [9] D.K. Sze, K. McCarthy, M. Sawan, M.S. Tillack, A. Ying, S. Zinkle, FLiBe assessments, *Fus. Technol.* 39 (2, Part 2) (2001) 746–749.
- [10] X-5 Monte Carlo Team, MCNP—A general Monte Carlo n-particle transport code, version 5, vol. II: Users Guide, LA-CP-03-0245, Los Alamos National Laboratory 2003.
- [11] DANTSYS: A Diffusion Accelerated Neutral Particle Transport Code System, Los Alamos National Laboratory, LA-12969-M, June, 1995.
- [12] M. Herman, H. Wienke, FENDL/MG-2.0 and FENDL/MC-2.0, the processed cross-section libraries for neutron-photon transport calculations, Report IAEA-NDS-176, International Atomic Energy Agency, March, 1997.
- [13] L. El-Guebaly, Nuclear issues and analysis for ARIES spherical and advanced tokamaks, *Fus. Eng. Des.* 51–52 (2000) 325–330.
- [14] F. Najmabadi, C. Bathke, M. Billone, J. Blanchard, L. Bromberg, E. Chin, et al., Overview of ARIES-RS reversed shear power plant study, *Fus. Eng. Des.* 38 (1997) 3–25.
- [15] C.E. Kessel, T.K. Mau, S.C. Jardin, F. Najmabadi, Plasma profile and shape optimization for the advanced tokamak power plant, ARIES-AT, *Fus. Eng. Des.* 80 (2006) 63–77.
- [16] F. Dahlgren, T. Brown, P. Heitzenroeder, L. Bromberg and The ARIES Team, ARIES-AT magnet system, *Fus. Eng. Des.* 80 (2006) 139–160.
- [17] L. Bromberg, M. Tekula, L. El-Guebaly, R. Miller, Options for the use of high temperature superconductor in toka-

- mak fusion power plant, *Fus. Eng. Des.* 54 (2001) 167–180.
- [18] L.M. Waganer, F. Najmabadi, M.S. Tillack, X. Wang, L.A. El-Guebaly, Design approach of the ARIES-AT power core and vacuum vessel cost assessment, *Fus. Eng. Des.* 80 (2006) 181–200.
- [19] D.A. Petti, B.J. Merrill, R.L. Moore, G.R. Longhurst, L. El-Guebaly, E. Mogahed, et al., ARIES-AT safety design and analysis, *Fus. Eng. Des.* 80 (2006) 111–137.
- [20] R. Klueh, M.L. Grossbeck, E.E. Bloom, Impurity content of reduced-activation ferritic steels and vanadium alloy, Fusion Materials Semiannual Progress Report for Period Ending December 31, 1996, U.S. Department of Energy Office of Fusion Energy Sciences, DOE/ER-0313/21, April, 1997.
- [21] G.R. Odette, D.T. Hoelzer, Development of nanocomposited ferritic alloys for high performance fusion first wall and blanket structures, ANS-FED Newsletter, June 2002. Available at: <http://fed.ans.org/>.
- [22] E. Mogahed, L. El-Guebaly, A. Abdou, P. Wilson, D. Henderson, Loss of coolant and loss of flow accident analyses for ARIES-AT power plant, *Fus. Technol.* 39 (2) (2001) 462–466.
- [23] W. Daenner, Max-Planck-Institut für Plasmaphysik, Garching, Germany, private communications, March 2000.
- [24] L. El-Guebaly, D. Henderson, A. Abdou, P. Wilson, Clearance issues for advanced fusion power plants, *Fus. Technol.* 39 (2) (2001) 986–990.
- [25] ARIES systems code outputs. Available at ARIES web site: <http://aries.ucsd.edu>.